Effect of intrapulse stimulated Raman scattering on soliton-effect pulse compression in optical fibers

Govind P. Agrawal

The Institute of Optics, University of Rochester, Rochester, New York 14627

Received September 22, 1989; accepted December 15, 1989

The effect of intrapulse stimulated Raman scattering (ISRS) on the quality of soliton-effect pulse compression is analyzed by solving the generalized nonlinear Schrödinger equation numerically. The results show that ISRS can improve the performance of soliton-effect pulse compressors both qualitatively and quantitatively. The compressed pulse is shorter with a higher peak power when ISRS is taken into account. Furthermore it is pedestal free as it separates from the background. The separation is due to the soliton self-frequency shift initiated by the process of ISRS. It can also be understood in terms of the soliton decay. The optimum fiber length is found to be longer than that expected in the absence of ISRS.

The use of optical fibers for pulse compression has become widespread in recent years.[1] Two distinct compression schemes are used, depending on whether the pulse experiences normal or anomalous group-velocity dispersion (GVD) inside the fiber. In the case of normal GVD the fiber imposes a nearly linear frequency chirp across the pulse, which is subsequently compressed by passing it through a grating pair.[1–3] In the case of anomalous GVD the pulse is chirped and compressed by the same fiber, and the compression mechanism is related to the evolution of high-order solitons in optical fibers. Such solitons undergo an initial pulse-narrowing state during their periodic evolution. By a judicious choice of the fiber length, the pulse can be made to exit from the fiber when it is narrowest.[4] This technique is referred to as the soliton-effect compression technique to emphasize its origin. The optimum fiber lengths and the compression factors have been obtained by solving the nonlinear Schrödinger equation.[4]

The predictions of the nonlinear Schrödinger equation are accurate for picosecond pulses but need to be modified for femtosecond input pulses, as several higher-order nonlinear effects become important for such short pulses. The most important among them is intrapulse stimulated Raman scattering[5] (ISRS), a phenomenon responsible for the soliton self-frequency shift[6,7] and soliton decay.[8,9] Dianov *et al.*[5] observed ISRS (also called self-induced Raman scattering). Mitschke and Mollenauer[6] observed the soliton self-frequency shift, and Gordon[7] interpreted it as an effect caused by ISRS. Physically, when the spectral width exceeds a few terahertz, the high-frequency components of the pulse can pump the low-frequency components of the same pulse through ISRS. Such pumping results in a gradual shift of the pulse spectrum toward longer wavelengths as the pulse propagates inside the fiber. It also destroys the periodic evolution pattern of high-order optical solitons. One would expect ISRS to affect the optimum fiber length and the compression factor realized by using the soliton-effect compression technique. Indeed, it was noted in several experiments[10] that the optimum fiber length did not agree with the prediction of the nonlinear Schrödinger equation for ultrashort pulses. The objective of this Letter is to evaluate numerically the effect of ISRS on the performance of soliton-effect pulse compressors.

With the inclusion of the higher-order nonlinear effects, pulse propagation in optical fibers is governed by a generalized nonlinear Schrödinger equation.[7–11] In the normalized coordinates commonly used for describing optical solitons, this equation takes the form[12]

$$i\frac{\partial U}{\partial \xi}+\frac{1}{2}\frac{\partial^2 U}{\partial \tau^2}-i\delta\frac{\partial^3 U}{\partial \tau^3}=$$

$$-N^2\left[|U|^2U+is\frac{\partial}{\partial \tau}(|U|^2U)-\tau_R U\frac{\partial}{\partial \tau}(|U|^2)\right], \quad (1)$$

where U is the normalized complex amplitude of the pulse envelope and

$$\xi=\frac{|\beta_2|z}{T_0^2}, \qquad \tau=\frac{t-z/v_g}{T_0}, \qquad N^2=\frac{n_2\omega_0 P_0 T_0^2}{cA_{\text{eff}}|\beta_2|}, \quad (2)$$

$$\delta=\frac{\beta_3}{6|\beta_2|T_0}, \qquad s=\frac{2}{\omega_0 T_0}, \qquad \tau_R=\frac{T_R}{T_0}. \quad (3)$$

In Eqs. (2) and (3) β_2 is the GVD coefficient (assumed to be negative), β_3 is the third-order dispersion coefficient, v_g is the group velocity, n_2 is the nonlinearity coefficient ($n_2 \simeq 3.2\times10^{-20}$ m^2/W for silica fibers), ω_0 is the optical frequency, c is the velocity of light, A_{eff} is the effective core area, P_0 is the peak power of the input pulse, and T_0 is the pulse width.

The parameters δ, s, and τ_R take into account, respectively, the effects of higher-order dispersion, self-steepening, and ISRS. For relatively wide pulses ($T_0 \gg 1$ psec), these parameters are negligible, and Eq. (1) reduces to the conventional nonlinear Schrödinger equation that governs the evolution of optical solitons. In particular, for input pulses having an amplitude

$$U(0,\tau)=N\,\text{sech}(\tau), \quad (4)$$

with N as an integer, the evolution pattern is periodic

0146-9592/90/040224-03$02.00/0

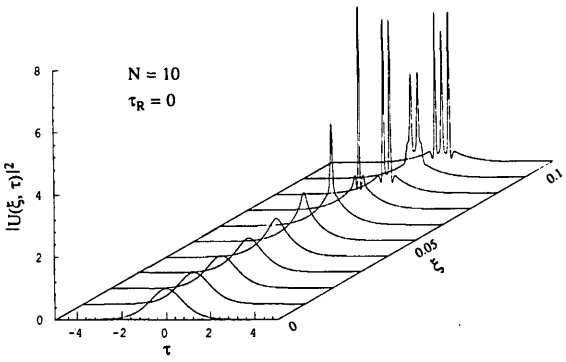

Fig. 1. Evolution of the tenth-order soliton over the range ξ = 0–0.1 showing pulse narrowing and splitting associated with higher-order solitons. ISRS is neglected by setting τ_R = 0.

with the soliton period $\xi_0 = \pi/2$. The fundamental soliton corresponds to $N = 1$ and propagates without change in its shape. The higher-order solitons ($N > 1$) change their shape but recover periodically at multiples of the soliton period. During each period they pass through an initial pulse-narrowing stage that is used for pulse compression.

For ultrashort optical pulses ($T_0 < 1$ psec) the higher-order terms in Eq. (1) are not negligible and begin to influence pulse evolution more and more as the pulse becomes shorter and shorter. It turns out that the ISRS, governed by the parameter τ_R, plays the dominant role, while the effects of higher-order dispersion (the term containing δ) and self-steepening (the term containing s) are important only for pulses much shorter than 100 fsec. To provide an estimate of the three parameters τ_R, δ, and s, we consider a 1.55-μm hyperbolic-secant pulse with a FWHM of T_{FWHM} = 1 psec. The parameter T_R is estimated from the Raman gain spectrum[7] to be approximately 6 fsec. The parameter T_0 is obtained using the general relation $T_{\mathrm{FWHM}} \simeq 1.76T_0$ and is 570 fsec. The ratio $\tau_R = T_R/T_0$ is thus approximately 0.01. Using typical values of β_2 and β_3 for silica fibers near 1.55 μm, we have $\delta \simeq 1.5 \times 10^{-3}$ and $s = 2.6 \times 10^{-3}$. The three parameters scale inversely with the pulse width as seen in Eqs. (3). Thus for a 100-fsec (FWHM) pulse these parameters become $\tau_R = 0.1$, $\delta = 0.015$, and $s = 0.026$. Clearly the effects of ISRS are going to dominate in practice.

Equation (1) is solved numerically with initial condition (4) by using the split-step Fourier method.[13] For illustration, we consider a tenth-order soliton and choose $N = 10$. The qualitative behavior discussed below, however, remains the same for other values of N. Before considering the general case, it is useful to discuss the expected behavior when the higher-order terms are neglected in Eq. (1) by setting $\delta = s = \tau_R = 0$. Figure 1 shows the evolution of the tenth-order soliton over a range ξ = 0–0.1 for this specific case. The pulse develops a narrow central spike near $\xi = 0.07$ and then splits into several components. Since pulse evolution is periodic in this case, the input pulse shape is recovered at $\xi = \pi/2$ (not shown in Fig. 1). For the purpose of pulse compression, the fiber length is chosen to correspond to $\xi \simeq 0.07$. The output then consists of a narrow central spike riding on a broad pedestal. A shortcoming of this compression technique is that a large part of the input pulse energy is contained in the broad pedestal surrounding the compressed pulse; 70% of the pulse energy remains in the pedestal for N = 10.

We now consider how pulse evolution is affected when ISRS is taken into consideration. To be specific, we choose $\tau_R = 0.01$, $\delta = 0$, and $s = 0$. As discussed above, this value of τ_R corresponds to an input pulse width (FWHM) of approximately 1 psec. The parameters δ and s for such a pulse are so small that their effect on pulse evolution is negligible. With $\beta_2 \simeq -20$ psec^2/km, the dispersion length $L_D = T_0^2/|\beta_2| \simeq 18$ m. The physical length is thus obtained by multiplying ξ by 18 m.

Figure 2 shows pulse evolution under conditions identical to those of Fig. 1 ($N = 10$) except that ISRS is accounted for by taking $\tau_R = 0.01$. The pulse shapes are nearly identical in the two cases up to approximately $\xi = 0.06$ except for a slight asymmetry. ISRS, however, leads to a drastic change in pulse shapes for $\xi \geq 0.07$. The most notable feature is that the narrow spike separates from the main pulse and moves toward the right in Fig. 2. This spike corresponds to the central spike in Fig. 1 seen at $\xi = 0.07$. Whereas the central spike disintegrates into a multiple-peak pattern for $\xi > 0.07$ when $\tau_R = 0$, it remains intact and shifts to the right in the case of $\tau_R = 0.01$. Physically the spike moves slower than the rest of the pulse and is delayed with an increase in the propagation distance.

To understand the delay of the spike from the rest of the pulse, it is useful to consider how the pulse spectrum changes in the presence of ISRS. Figure 3 shows the pulse spectrum at $\xi = 0.08$. As expected, ISRS transfers pulse energy to the red side, resulting in an asymmetric pulse spectrum. The red-shifted spectral peak centered at $\Delta\nu \simeq -9/T_0$ is due the soliton self-frequency shift initiated by ISRS.[5–7] The narrow spike seen in Fig. 2 is associated with this red-shifted spectral peak. The delay of the spike results from a combination of the self-frequency shift and anoma-

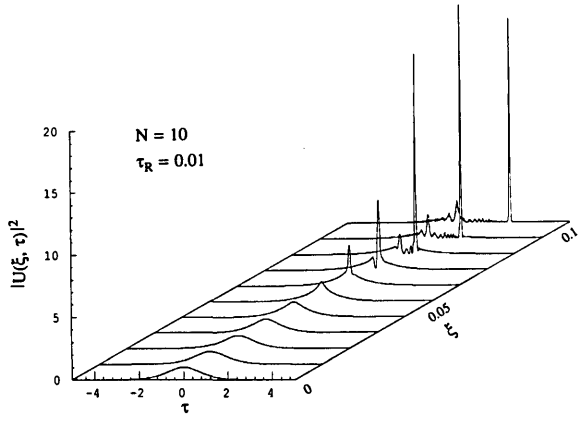

Fig. 2. Same as in Fig. 1 except that ISRS is included by choosing $\tau_R = 0.01$. This value of τ_R is appropriate for a 1-psec input pulse. The propagation distance is $\xi = z/L_D$, where L_D is estimated to be 18 m for a 1-psec pulse propagating in a fiber with $\beta_2 = -20$ psec^2/km.

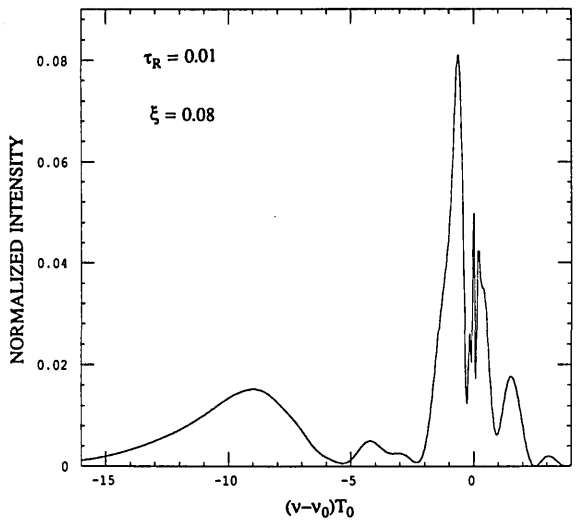

Fig. 3. Pulse spectrum at $\xi = 0.08$ for $\tau_R = 0.01$ showing the development of a red-shifted spectral peak as a result of ISRS.

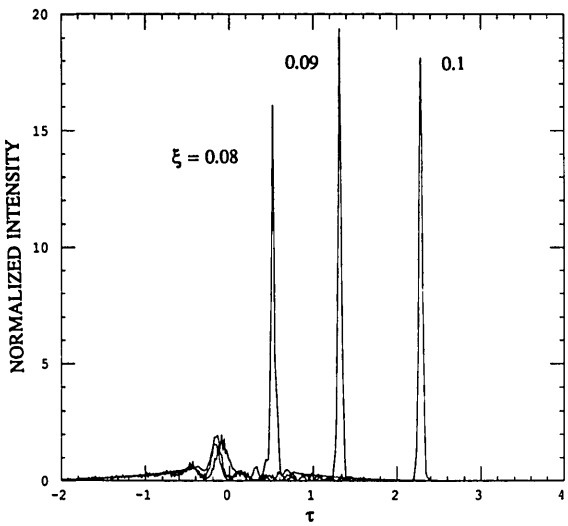

Fig. 4. Pulse shapes at $\xi = 0.08$, 0.09, and 0.1 showing separation of the compressed spike from the rest of the pulse.

lous GVD. In the presence of anomalous GVD the red-shifted components travel slower than the rest of the pulse and take longer to arrive. This is precisely what is seen in Fig. 2, where the spike is delayed and breaks away from the rest of the pulse. Figure 4 compares the pulse shapes $\xi = 0.08$, 0.09, and 0.1. The spike is completely separated from the rest of the pulse at $\xi = 0.1$. The spike width is reduced by more than a factor of 90 compared with the input pulse width. The peak power is largest near $\xi = 0.09$.

From a practical standpoint the narrow spike corresponds to the compressed pulse. The results show that higher-order solitons provide a pulse-compression mechanism even when the input pulses are so short that the periodic evolution of such solitons along the fiber ceases to occur because of ISRS. In fact, ISRS is beneficial to the overall quality of pulse compression. This can be seen by comparing Figs. 1 and 2. The compression factor and the peak power are considerably larger for $\tau_R = 0.01$ than for $\tau_R = 0$. More importantly, the compressed pulse no longer rides on a broad pedestal but is physically separated from the background as a result of the soliton self-frequency shift. The optimum fiber length for maximum compression is longer than that expected when ISRS is neglected by setting $\tau_R = 0$. This is in agreement with recent experiments.[10]

This Letter has discussed the role of ISRS on the quality of pulse compression occurring in the anomalous GVD regime of optical fibers. In the absence of ISRS, the input pulse evolves toward a higher-order soliton and passes through an initial stage in which a narrow central spike develops over a broad pedestal. The spike corresponds to the compressed pulse, but the quality of pulse compression is poor as a large fraction of the input energy appears in the form a broad pedestal. These results show that ISRS can improve the performance of soliton-effect pulse compressors both qualitatively and quantitatively. In particular, the compressed pulse separates from the background as it travels slower than the rest of the pulse. The separation is due to the soliton self-frequency shift initiated by the process of ISRS.[5–7] It can also be understood in terms of the soliton decay.[8,9] The bound state of a higher-order soliton no longer remains stable in the presence of ISRS, and the multisoliton pulse decays into its individual components. Although the numerical results for a specific value of τ_R have been presented, the qualitative behavior is found to be the same over a large range of τ_R. In particular, soliton decay occurs for a value of τ_R as small as 0.001, a value that is appropriate for a 10-psec input pulse.

This research is supported by the U.S. Army Research Office and by the Joint Services Optics Program.

References

1. For a recent review see G. P. Agrawal, *Nonlinear Fiber Optics* (Academic, Boston, Mass., 1989), Chap. 6.
2. A. S. L. Gomes, A. S. Gouveia-Neto, and J. R. Taylor, Opt. Quantum Electron. **20,** 95 (1988).
3. E. A. Golovchenko, E. M. Dianov, P. V. Mamyshev, and A. M. Prokhorov, Opt. Quantum Electron. **20,** 343 (1988).
4. L. F. Mollenauer, R. H. Stolen, J. P. Gordon, and W. J. Tomlinson, Opt. Lett. **8,** 289 (1983).
5. E. M. Dianov, A. Ya Karasik, P. V. Mamyshev, A. M. Prokhorov, V. N. Serkin, M. F. Stelmakh, and A. A. Fomichev, JETP Lett. **41,** 294 (1985).
6. F. M. Mitschke and L. F. Mollenauer, Opt. Lett. **11,** 659 (1986).
7. J. P. Gordon, Opt. Lett. **11,** 662 (1986).
8. E. A. Golovchenko, E. M. Dianov, A. M. Prokhorov, and V. N. Serkin, JETP Lett. **42,** 87 (1985).
9. K. Tai, A. Hasegawa, and N. Bekki, Opt. Lett. **13,** 392 (1988).
10. A. S. Gouveia-Neto, A. S. L. Gomes, and J. R. Taylor, Opt. Lett. **12,** 395 (1987).
11. Y. Kodama and A. Hasegawa, IEEE J. Quantum Electron. **QE-23,** 510 (1987).
12. Sections 2.3 and 5.5 of Ref. 1.
13. The split-step Fourier method is also known as the beam-propagation method. See Sec. 2.4 of Ref. 1 and references therein for details of the numerical method.